

# LARGE EDDY SIMULATION OF CONVECTIVE ENTRAINMENT IN LINEARLY AND DISCRETELY STRATIFIED FLUIDS

Evgeni Fedorovich and Robert Conzemius

*School of Meteorology, University of Oklahoma, Norman OK 73019, USA*  
fedorovich@ou.edu

**Abstract** Regimes of convective entrainment in linearly and discretely stratified fluids are investigated by means of a high-resolution LES in conjunction with relevant data from atmospheric, laboratory, numerical, and analytical studies of penetrative convection. Relationships between parameters of entrainment in the discretely stratified fluid are shown to be rather different to their counterparts in the case of equilibrium entrainment in the linearly stratified fluid.

**Keywords:** boundary layer, buoyancy, convection, entrainment, stratified fluid

## 1. Introduction

Boundary layers driven by surface buoyant forcings are rather typical for the environmental flows. An atmospheric example of such boundary layer is the so-called convective boundary layer (CBL), which is driven by buoyancy production at the heated underlying surface of the earth during the daytime conditions. The CBL develops in the stably stratified environment of the earth atmosphere. In many instances, the buoyancy production of turbulence in the atmospheric CBL considerably dominates its production due to flow (wind) shears, so the CBL can be considered shear-free. The buoyancy is defined as  $b = -g(\rho - \rho_0)/\rho_0$ , where  $\rho$  is the density of the fluid,  $\rho_0$  is the reference density, and  $g$  is the acceleration due to gravity. In atmospheric terms, the buoyancy can be approximately expressed as  $b = g(\theta_v - \theta_{v0})/\theta_{v0}$ , where  $\theta_v$  is the virtual potential temperature.

The buoyant convective forcing generates up- and downward motions that effectively mix buoyancy (virtual potential temperature) field inside the CBL. In meteorology, the convective upward motions (updrafts) are commonly referred to as thermals. The warm and fast rising thermals occupy less percentage of the CBL horizontal cross-sectional area than broader, but slower and cooler, descending convective downdrafts. Due to mixing

associated with convective up- and downdrafts, the buoyancy field in the main portion of the CBL (the so-called convectively mixed layer) does not change considerably with height when averaged over horizontal planes or over time. Relatively large vertical gradients in the averaged buoyancy profile are observed close to the CBL top, throughout the interfacial (sub)layer that separates CBL from the stably stratified atmosphere aloft. A more buoyant air from the free atmosphere is entrained across this interfacial layer (also called the capping inversion layer, or simply - capping inversion) into the convectively mixed flow region as the CBL grows. Such convective entrainment is maintained by flow disturbances resulting from the penetration of convective thermals into the stably stratified fluid above the CBL.

The CBL growth rate and the entrainment dynamics essentially depend on the stratification of quiescent fluid (free atmosphere), in which the CBL grows. This stratification can be continuous as well as discrete in the vertical. The particular case of continuous linear stratification corresponds to a constant buoyancy (virtual potential temperature) gradient in the fluid above the density interface. The discrete stratification is characteristic of a multilayer fluid with discontinuities of the buoyancy gradient at the interfaces between layers.

During several recent years, the numerical large eddy simulation (LES) has been extensively applied to study convective entrainment in the continuously and linearly stratified atmosphere with and without wind shears, see review in Stevens and Lenschow (2001). However, even for the case of shear-free CBL, a consensus has not been reached so far regarding the dependence of the integral parameters of entrainment on the capping inversion strength and stability in the quiescent fluid above the CBL. These integral parameters are the CBL growth rate (also called the entrainment rate), the entrainment ratio (the ratio of the heat flux of entrainment to the surface heat flux), and the relative entrainment layer depth (the ratio of the of entrainment layer depth to that of the CBL). Previous numerical studies of convective entrainment have often been handicapped by resolution and domain size limitations, which to date have prevented investigations of parameter variations over sufficiently wide ranges of free-atmosphere stratification and CBL depth.

Convective entrainment in a heterogeneously (*e.g.*, discretely or nonlinearly) stratified atmosphere has been studied much less. There is evidence, however, both from atmospheric observations (Nelson et al. 1989) and numerical bulk models of the CBL (Fedorovich and Mironov 1995) that the nonstationarity of the entrainment process plays an important role in this case, and the CBL evolution passes through a sequence of transition regimes accompanied by strong variations of entrainment parameters.

In the present study, regimes of convective entrainment in linearly and discretely stratified fluids have been investigated by means of a high-resolution LES in conjunction with relevant data from atmospheric, laboratory, numerical, and analytical studies of penetrative convection.

## 2. Employed LES technique

Following the established LES methodology, described *e.g.* in Lesieur and Métais (1996), turbulent motions in the simulated flow are subdivided into the larger-scale resolved motions that are directly reproduced on the computational grid, and the smaller-scale, the so-called subgrid motions, that are modeled through additional terms in the governing equations for the resolved quantities:

$$\frac{\partial \bar{u}_i}{\partial t} + \frac{\partial \bar{u}_j \bar{u}_i}{\partial x_j} = -\frac{\partial \pi}{\partial x_i} + \bar{b} \delta_{i3} + \frac{\partial}{\partial x_j} \left[ \nu \left( \frac{\partial \bar{u}_i}{\partial x_j} + \frac{\partial \bar{u}_j}{\partial x_i} \right) - \overline{u_i u_j} - \bar{u}_i \bar{u}_j \right], \quad (1)$$

$$\frac{\partial \bar{u}_i}{\partial x_i} = 0, \quad (2)$$

$$\frac{\partial \bar{b}}{\partial t} + \frac{\partial \bar{u}_i \bar{b}}{\partial x_i} = \frac{\partial}{\partial x_i} \left[ \mu \frac{\partial \bar{b}}{\partial x_i} - \overline{b u_i} - \bar{b} \bar{u}_i \right], \quad (3)$$

where  $i, j=1, 2, 3$ ;  $t$  stands for the time,  $x_i = (x, y, z)$  are the right-hand Cartesian coordinates,  $\bar{u}_i = (\bar{u}, \bar{v}, \bar{w})$  are the resolved-scale components of the velocity vector,  $\bar{b}$  is the resolved-scale buoyancy,  $\nu$  is the kinematic viscosity, and  $\mu$  is the molecular thermal diffusivity. The quantities  $\overline{u_i u_j} - \bar{u}_i \bar{u}_j$  and  $\overline{b u_i} - \bar{b} \bar{u}_i$  are the components of the subgrid stress and subgrid buoyancy flux, respectively. The overbar signifies the grid-cell volume average, which in our case is taken to be the filter procedure for separation of the resolved-scale motions from the subgrid-scale ones. The normalized pressure  $\pi$  is defined as  $\pi = (\bar{p} - p_0) / \rho_0$ , where  $\bar{p}$  is the resolved pressure, whilst  $p_0$  and  $\rho_0$  are the reference values of pressure and density, respectively. In (1), the Boussinesq approximation is used to account for the buoyancy forcing, and the Coriolis force, which is not important in the shear-free atmospheric CBL, is neglected.

The subgrid stress and buoyancy flux are parameterized in terms of an eddy viscosity/diffusivity model of Deardorff (1980):

$$\overline{u_i u_j} - \bar{u}_i \bar{u}_j = \frac{2}{3} E \delta_{ij} - 2K_m s_{ij}, \quad (4)$$

$$\overline{b u_i} - \bar{b} \bar{u}_i = -K_h \frac{\partial \bar{b}}{\partial x_i}, \quad (5)$$

where  $s_{ij} = \frac{1}{2} \left( \frac{\partial \bar{u}_i}{\partial x_j} + \frac{\partial \bar{u}_j}{\partial x_i} \right)$  is the deformation tensor of the filtered velocity

field,  $K_m$  and  $K_h$  are the subgrid-scale eddy diffusivities for momentum and heat, respectively, and  $E$  is the subgrid kinetic energy, which is determined from the following balance equation:

$$\frac{\partial E}{\partial t} + \frac{\partial \bar{u}_i E}{\partial x_i} = 2K_m s_{ij} \frac{\partial \bar{u}_i}{\partial x_j} - K_h \frac{\partial \bar{b}}{\partial x_3} + \frac{\partial}{\partial x_i} 2K_m \frac{\partial E}{\partial x_i} - \varepsilon, \quad (6)$$

where  $\varepsilon$  stands for the viscous dissipation rate. The eddy diffusivities are expressed through the mixing length  $l$  and  $E$  as

$$K_m = 0.12lE^{1/2}, \quad K_h = (1 + 2l/\Delta)K_m, \quad (7)$$

where  $\Delta = (\Delta x \Delta y \Delta z)^{1/3}$  is the effective grid cell size, and  $\varepsilon$  is parameterized as

$$\varepsilon = f_c [0.19 + 0.51(l/\Delta)] (E^{3/2}/l), \quad (8)$$

where  $f_c$  is the correction multiplier varying with distance from the wall (Nieuwstadt 1990). The subgrid mixing length  $l$  is evaluated depending on the local buoyancy gradient in the following manner:

$$l = \Delta \quad \text{if } \partial \bar{b} / \partial z \leq 0, \quad l = \min\{\Delta, 0.5E^{1/2} / (\partial \bar{b} / \partial z)^{1/2}\} \quad \text{if } \partial \bar{b} / \partial z > 0. \quad (9)$$

Equations (1)-(9) are discretized on a staggered grid in the rectangular computational domain. The domain size and the number of grid cells may vary. In the reported study, the domain size was 5km×5km×4km, where the last dimension is the vertical one, and grid consisted of 50×50×200 rectangular cells of uniform size. A few test runs have been performed on a 100×100×200 grid.

The spatial discretization on the grid is of the second order in space. The time advancement is carried out by means of the leapfrog explicit time integration scheme with a weak time filter. Enforcement of the mass conservation in the simulated flow is realized by the pressure. A Poisson equation for  $\pi$  is constructed by combining the continuity and momentum balance equations as it is done in Nieuwstadt (1990). This Poisson equation is solved numerically by the fast Fourier-transform technique over the horizontal planes, and by tridiagonal matrix decomposition in the vertical. For the pressure field, the Neumann boundary conditions are set at all boundaries of the domain.

At the sidewalls of simulation domain, periodic boundary conditions are prescribed for prognostic variables  $\bar{u}_i = (\bar{u}, \bar{v}, \bar{w})$ ,  $\bar{b}$ , and  $E$ . In the upper 20% fraction of the domain, the sponge layer is introduced in order to damp vertical motions close to the domain top and to ensure steady-state conditions at the upper boundary. To minimize the inevitable spurious influence of the sponge layer on the numerical solution, the time advancement is maintained only as long as the CBL depth is less than 60% of the domain height. The no-slip boundary condition for the velocity and zero-gradient condition for the subgrid energy are prescribed at the heated bottom surface. The Monin-Obukhov similarity relationships are used point by point to couple local buoyancy and mechanical turbulence forcings within the lowest layer of grid cells. The surface roughness length and buoyancy flux are prescribed as external parameters of the problem.

### 3. Convective entrainment in linearly stratified fluid

Figure 1 shows schematically the vertical structure of buoyancy  $b$  and vertical turbulent buoyancy flux  $B$  in a shear-free CBL, which grows by entrainment in a linearly stratified fluid heated from below. Three regions (sublayers) can be distinguished within the CBL: (i) a comparatively shallow surface layer, where  $b$  drops with height from a surface value to the mixed layer value; (ii) the convectively mixed layer, where  $b$  is approximately constant with height; and (iii) the capping inversion layer, where  $b$  sharply increases with height. The vertical buoyancy flux  $B$  decreases with height in the mixed layer and its zero-crossing height signifies the mixed layer top. Inside the inversion layer,  $B$  reaches a minimum at level  $z_i$  and vanishes towards its upper boundary. The fluid above the CBL is linearly stratified with the vertical buoyancy gradient  $db/dz=N^2$ , where  $z$  is the height and  $N$  is the Brunt-Väisälä (buoyancy) frequency.

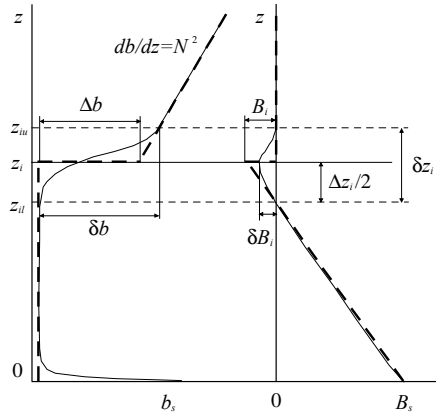


Figure 1. Approximation of the buoyancy  $b$  and buoyancy flux  $B$  profiles in a linearly stratified fluid according to the ZOI model, after Fedorovich and Mironov (1995). The actual profiles are shown by thin solid lines and the ZOI model profiles are given by heavy dashed lines. See text for the notation.

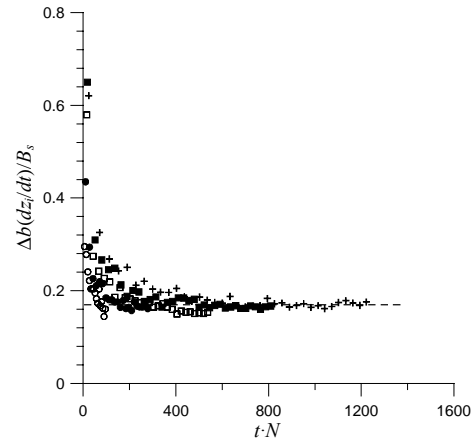


Figure 2. Entrainment coefficient in a linearly stratified fluid as function of dimensionless time. Symbols are the LES data for different  $N$  (open circles:  $N=0.008\text{s}^{-1}$ , filled circles:  $N=0.011\text{s}^{-1}$ , open squares:  $N=0.014\text{s}^{-1}$ , filled squares:  $N=0.016\text{s}^{-1}$ , crosses:  $N=0.018\text{s}^{-1}$ ). The dashed line shows the asymptotic value of entrainment coefficient ( $C_e=0.17$ ) as predicted by LES.

The convective entrainment in a linearly stratified atmosphere has been extensively studied using the zero-order jump (ZOJ) model (Lilly 1968). In this model, the inversion (or entrainment) layer is replaced by a zero-order discontinuity interface with buoyancy jump  $\Delta b$  at the level  $z_i$ . In the ZOI model, this level is taken as the CBL top, see Figure 1. Note that  $\Delta b$  is

generally smaller than the actual buoyancy increment  $\delta b$  across the entrainment layer of depth  $\delta z_i$ . The buoyancy flux of entrainment in the ZOI model is given by  $B_i = -\Delta b \cdot (dz_i/dt)$ , where  $t$  is the time. As indicated in Figure 1, this flux is not equal to the actual buoyancy flux of entrainment  $\delta B_i$  at level  $z_i$ .

The zero-order approach has been successfully applied to predict the entrainment rate  $dz_i/dt$  as related to  $z_i$ ,  $\Delta b$ ,  $N$ , and the surface buoyancy flux  $B_s$ . If the quantities  $\Delta b$ ,  $N$  and  $B_s$  are known, any reasonable assumption on  $B_i$  closes the problem, see Fedorovich and Mironov (1995).

The most comprehensive ZOI model of the shear-free CBL was proposed by Zilitinkevich (1991). Based on the assumption that  $t$ ,  $B_s$  and  $N$  are the only determining parameters of the entrainment regime in a linearly stratified fluid with constant bottom buoyancy flux, and neglecting energy drain by internal gravity waves at the CBL top, Zilitinkevich (1991) obtained the following analytical solutions for  $z_i$  and  $\Delta b$  in terms of  $N$ ,  $B_s$ , and  $t$ :

$$\hat{z}_i = [2(1 + 2C_\varepsilon)\hat{t}]^{1/2}, \quad \Delta\hat{b} = C_\varepsilon [2\hat{t}/(1 + 2C_\varepsilon)]^{1/2}. \quad (10)$$

where  $\hat{t} = tN$ ,  $\hat{z}_i = z_i B_s^{-1/2} N^{3/2}$ , and  $\Delta\hat{b} = \Delta b B_s^{-1/2} N^{-1/2}$  are the scaled time, CBL depth, and inversion-layer buoyancy increment, respectively, and  $C_\varepsilon$  is the dimensionless constant, which in the case under consideration equals to the entrainment coefficient, because:  $C_\varepsilon = (\Delta\hat{b} \cdot \hat{z}_i) / (2\hat{t}) = \Delta\hat{b} (d\hat{z}_i / d\hat{t}) = \Delta b (dz_i / dt) / B_s = -B_i / B_s$ . The ZOI model solutions (10) correspond to the regime of equilibrium entrainment at times  $\hat{t}$  that are sufficiently large to ensure the independence of  $\hat{z}_i$  and  $\Delta\hat{b}$  of their initial values. From analyses of atmospheric and laboratory data on convective entrainment Zilitinkevich (1991) retrieved  $C_\varepsilon = 0.2$ .

The above analytical expressions of  $\hat{z}_i = \hat{z}_i(\hat{t})$  and  $\Delta\hat{b} = \Delta\hat{b}(\hat{t})$  have been used to test the employed LES code. The tests have been conducted with surface buoyancy flux  $B_s = 0.0098 \text{ m}^2 \cdot \text{s}^{-3}$  and buoyancy frequency  $N$  within the range of its atmospheric variability (from 0 to  $0.018 \text{ s}^{-1}$ ). To facilitate the comparability with the analytical solution, the LES output data have been post-processed in terms of the ZOI model. Simulation results for  $C_\varepsilon = \Delta b (dz_i / dt) / B_s$  are presented in Figure 2.

As may be concluded from this plot, our LES code correctly predicts asymptotic behavior of  $C_\varepsilon$  in the regime of equilibrium entrainment and yields the asymptotic value of entrainment coefficient very close to its atmospheric and laboratory estimate  $C_\varepsilon = 0.2$ .

## 4. Convective entrainment in discretely stratified fluid

The case of continuous linear stratification in the fluid above the growing CBL corresponds to a rather idealized atmospheric situation. In reality, the vertical structure of the free atmosphere is quite heterogeneous. It can be considered as set of sublayers with different vertical extensions and density/buoyancy lapse rates. Atmospheric observations of Nelson *et al.* (1989) and CBL bulk model results of Fedorovich and Mironov (1995) provide grounds to assume that convective entrainment in such multilayer fluid system is an essentially nonstationary process that cannot be described by relationships between the entrainment parameters designed for equilibrium entrainment in a linearly stratified fluid.

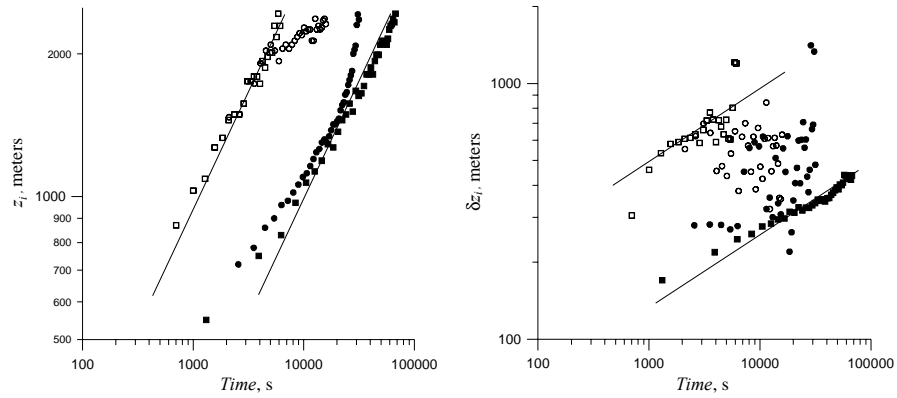


Figure 3. Evolution of the CBL depth (left plot) and the entrainment zone thickness (right plot) in the discretely versus linearly stratified fluid. The LES results for the linearly stratified fluid are presented by squares: open for  $N_w=0.005s^{-1}$  and filled for  $N_s=0.018s^{-1}$ . The open circles show LES results for the WS case (transition from  $N_w=0.005s^{-1}$  to  $N_s=0.018s^{-1}$ ) and the filled circles – for the SW case (transition from  $N_s=0.018s^{-1}$  to  $N_w=0.005s^{-1}$ ). The lines present power dependencies for the equilibrium entrainment: 1/2 for the CBL depth and 5/18 for the entrainment zone thickness.

We have conducted a series of LES runs in order to investigate transition regimes of convective entrainment in the fluid system consisting of differently stratified layers (we call this system the discretely stratified fluid). In the first investigated flow configuration (hereafter referred to as the WS case), the CBL first develops in a weakly stratified fluid (small  $N$ ) and then proceeds into the environment with a relatively strong stratification (large  $N$ ). The second investigated configuration (designated as the SW case) is somewhat opposite to the first one: the CBL initially grows in a strongly stratified fluid and then proceeds into a weaker stratified fluid. In both cases, the change of buoyancy lapse rate in the fluid above the CBL occurs abruptly at a prescribed elevation. The values of  $N$  in the weakly and strongly stratified fluids have been  $N_w=0.005s^{-1}$  and  $N_s=0.018s^{-1}$ , respectively.

Simulated time evolution of the CBL depth (represented by  $z_i$ ) and the entrainment zone thickness  $\delta z_i$  for the WS and SW cases are shown in Figure 3 together with reference LES data on convection in uniformly stratified fluids with  $N_w=0.005\text{s}^{-1}$  and  $N_s=0.018\text{s}^{-1}$ . One may notice that the reference dependencies  $z_i(t)$  and  $\delta z_i(t)$  have rather extended and pronounced intervals corresponding to the equilibrium entrainment regime. Our previous analytical considerations (see Eq. 10), supported by LES results and comparisons with experimental data (not shown) allow to conclude that in the equilibrium regime:  $z_i \sim t^{1/2}$  and  $\delta z_i \sim t^{5/18}$ .

Demonstrated LES data for the WS and SW cases clearly show that parameters of entrainment in the discretely stratified fluid can depend on time in a very different manner compared to the case of equilibrium entrainment. This anomalous behavior extends far beyond the transition point in the background stratification, which means that the adjustment of entrainment to the new environment happens rather slowly, at the time scales much larger than the CBL turnover time scale.

## References

- Deardorff, J. W., 1980: Stratocumulus-capped mixed layers derived from a three-dimensional model. *Bound.-Layer Meteor.*, **18**, 495-527.
- Fedorovich, E. E., and D. V. Mironov, 1995: A model for shear-free convective boundary layer with parameterized capping inversion structure. *J. Atmos. Sci.*, **52**, 83-95.
- Lesieur, M., and O. Métais, 1996: New trends in large-eddy simulations of turbulence. *Annu. Rev. Fluid Mech.*, **28**, 45-82.
- Lilly, D. K., 1968: Models of cloud-topped mixed layers under a strong inversion. *Quart. J. Roy. Meteorol. Soc.*, **94**, 292-309.
- Nelson, E., R. Stull, and E. Eloranta, 1989: A prognostic relationship for entrainment zone thickness. *J. Appl. Meteorol.*, **28**, 885-903.
- Nieuwstadt, F. T. M., 1990: Direct and large-eddy simulation of free convection. *Proc. 9th Internat. Heat Transfer Conference*, Jerusalem, Israel, 19-24 August 1990, Amer. Soc. Mech. Engrg., New York, **1**, 37-47.
- Stevens, B., and D. H. Lenschow, 2001: Observations, experiments, and large eddy simulation. *Bull. Amer. Meteor. Soc.*, **82**, 283-294.
- Zilitinkevich, S.S., 1991: *Turbulent Penetrative Convection*. Avebury Technical, Aldershot, 179 pp.